Single-molecule-sensitive fluorescence resonance energy transfer in freely-diffusing attoliter droplets

Sheema Rahmanseresht, Peker Milas, Kieran P. Ramos, Ben D. Gamari, and Lori S. Goldner

Citation: Applied Physics Letters **106**, 194107 (2015); doi: 10.1063/1.4921202
View online: http://dx.doi.org/10.1063/1.4921202
View Table of Contents: http://scitation.aip.org/content/aip/journal/apl/106/19?ver=pdfcov
Published by the AIP Publishing

Single-molecule-sensitive fluorescence resonance energy transfer in freely-diffusing attoliter droplets

Sheema Rahmanseresht,[1] Peker Milas,[2] Kieran P. Ramos,[1] Ben D. Gamari,[1] and Lori S. Goldner[1,a)]
[1]Department of Physics, University of Massachusetts, Amherst, Massachusetts 01003, USA
[2]Department of Neuroscience, University of Wisconsin, Madison, Wisconsin 53705, USA

(Received 18 January 2015; accepted 5 May 2015; published online 15 May 2015)

Fluorescence resonance energy transfer (FRET) from individual, dye-labeled RNA molecules confined in freely-diffusing attoliter-volume aqueous droplets is carefully compared to FRET from unconfined RNA in solution. The use of freely-diffusing droplets is a remarkably simple and high-throughput technique that facilitates a substantial increase in signal-to-noise for single-molecular-pair FRET measurements. We show that there can be dramatic differences between FRET in solution and in droplets, which we attribute primarily to an altered pH in the confining environment. We also demonstrate that a sufficient concentration of a non-ionic surfactant mitigates this effect and restores FRET to its neutral-pH solution value. At low surfactant levels, even accounting for pH, we observe differences between the distribution of FRET values in solution and in droplets which remain unexplained. Our results will facilitate the use of nanoemulsion droplets as attoliter volume reactors for use in biophysical and biochemical assays, and also in applications such as protein crystallization or nanoparticle synthesis, where careful attention to the pH of the confined phase is required. © *2015 AIP Publishing LLC*. [http://dx.doi.org/10.1063/1.4921202]

Single-molecular-pair fluorescence resonance energy transfer (spFRET) is widely used in molecular biophysics to understand folding, binding, and structural changes in proteins[1] and RNA.[2] In the simplest and most frequently used application of spFRET, fluorescent photons are detected as a molecule diffuses through a femtoliter-volume confocal detection region. The number of photons detected depends on the brightness of the molecule and length of time spent (dwell time) in the detection volume, typically <1 ms. To some extent, the dwell time, and therefore the signal, can be increased by adding sucrose or glycerol to increase the viscosity of the solution. An increase in the detection volume also increases the dwell time, but the gain in signal is offset by a concurrent increase in background that limits this option.

Alternatively, the dwell time of a biomolecule can be dramatically increased, and the background minimized, by confinement in a nanocontainer that is larger than the biomolecule but smaller than the detection volume. Two common candidates for molecular confinement are droplets[3] and liposomes;[4] their relative merits have been discussed elsewhere.[5] It has long been assumed that confinement does not perturb FRET measurements; here we test that assumption for molecules confined in water-in-perfluorinated-liquid nanodroplets.

The Stokes-Einstein diffusivity for a spherical particle is $D = k_B T/6\pi\eta r$, where r is the hydrodynamic radius of the particle, k_B is the Boltzmann constant, T is the temperature, and η is the dynamic viscosity. The dwell time $\tau \propto w^2/D$ where w is the waist of the confocal detection volume (260 nm), so that τ scales with the radius of the particle and the viscosity of the medium. The droplets used in this study had a log-normal size distribution, with $\langle r \rangle = 101$ nm–135 nm as measured both by absorption (Mie scattering) and dynamic light scattering (DLS). For a typical sample, $\langle r \rangle = 118 \pm 10$ nm with 95% of droplets between $r = 76$ nm and $r = 175$ nm. Corresponding volumes were 1.8 aL–22 aL with a mean of 6.9 aL, resulting in $\tau \approx 12$ ms for droplets in FC-77 (Flourinert, 3M) and $\tau \approx 38$ ms for droplets in FC-40 (Flourinert, 3M); this should be compared with a $\tau \approx 375\,\mu$s for a molecule with $\langle r \rangle = 5$ nm in water.

At a nominal concentration ≤ 20 nM, 6.9 aL droplets contain ≈ 0.08 molecules on average, and the probability of finding more than 1 molecule in a droplet is ≤ 0.003. Empty droplets are not detected. Biomolecules confined in these droplets have been observed to rotate freely[6,7] and show no evidence of sticking at the perfluorinated boundaries (Fig. S1).[8] This observation does not rule out more subtle interactions with the boundary.

The confined molecule is 16-base-pair duplex RNA (IDT), with Cy3 and Cy5 (Glen Research) at the 5′ termini,[9] prepared in 20 mM Tris with 200 mM NaCl. For measurements on RNA unconfined in solution, the buffer contained 50 or 100 pM dsRNA with 100 nM protocatechuate-3,4-dioxygenase (PCD) and 2 mM protocatechuic acid (PCA) for oxygen getting[10] and 1 mM methylviologen (MV) for triplet quenching. For use in droplets, the buffer was prepared at pH 7.8, and contained dsRNA at 10 or 20 nM with 10 mM PCA, 50 nM PCD, and 1 mM MV. Droplets were formed by adding 2 μl of this RNA-containing buffer solution to 200 μl of a continuous phase consisting of degassed Fluorinert[8] with a triblock copolymer surfactant [perfluoro polyether (PFPE)–polyethylene glycol–PFPE, RainDance][11] at a concentration of 0.1%–2% (w/w). After shaking, the mixture was placed in an ultrasonic bath (Branson 1510) for 2–4 min, forming an emulsion. For all measurements, $\approx 50\,\mu$l of sample was withdrawn and placed between a coverslip and

a)Electronic mail: lgoldner@physics.umass.edu

microscope slide separated by double-sided sticky tape, which was sealed with grease or wax. Data were acquired on an Olympus IX50 microscope modified for single-molecule confocal detection with a 50 μm pinhole. A UPlanSApo 60×, 1.2 NA water immersion objective was used for fluorescence excitation and collection of emitted photons. The donor dye (Cy3) was excited at 514 nm (Argon-Krypton laser) with a nominal power at the scope entrance of 50 μW. Fluorescent photons were split into two channels (donor and acceptor) and detected using single-photon-counting avalanche photodiodes (τ-SPAD by Picoquant). Photon timing information was recorded with 8 ns resolution.[12]

A comparison of fluorescence from RNA unconfined in solution to RNA confined in droplets is shown in Fig. 1. Photons in the donor and acceptor channels are binned in 5 ms intervals and plotted in blue and red, respectively. The smaller panels on the right are 0.5 s expansions of the data colored black in the left panel. The peaks correspond to molecules diffusing across the detection volume. As expected, $\tau \ll 5$ ms for RNA in solution, Fig. 1(a), so the peaks typically consist of only one or two above-background bins. For molecules confined in aqueous droplets in FC-77, Fig. 1(b), or FC-40, Fig. 1(c), τ is substantially larger, with many more photons detected. Fluorescence correlation spectroscopy was used to confirm that the dwell times were consistent with the predictions of Stokes-Einstein.

In FRET, an excited donor dye transfers its energy to a redder acceptor dye with an efficiency given by $E = [1 + (R/R_F)^6]^{-1}$, where R is the distance between dyes and the Förster radius $R_F \approx 5.8$ nm for this system at neutral pH.[9] Following convention,[13] we report the histogram of the closely related proximity ratio

$$P = \frac{N_A}{N_A + N_D}, \tag{1}$$

where N_A and N_D are the number of photons in the acceptor and donor channels, respectively, in a given bin. P differs from E only due to background, crosstalk, and differences in quantum yield or collection efficiency of the two dyes.[13] Defining $N_t = N_A + N_D$, proximity histograms are formed using all bins with N_t greater than a threshold, N_{th}, given below.

Proximity ratio histograms for a bin time of 2 ms are shown in Fig. 2. Histograms were fit with the sum of three beta probability distribution functions (PDFs). The donor-only population, with $\langle P \rangle \approx 0.15$ due to crosstalk, was removed by sampling.[8] The best fit to the FRET peaks and the component beta PDFs are plotted with black and grey lines, respectively. Fit parameters and peak statistics are given in Table I.

The proximity histogram for RNA unconfined in solution at pH 7.8 with $N_{th} = 25$ is shown in Fig. 2(a). Data taken at pH 7.8 were indistinguishable from pH 7.0. It is not possible to substantially increase the threshold from $N_{th} = 25$; only 138 bins have $N_t \geq 50$.

Figs. 2(b)–2(d) are the proximity histograms for RNA in droplets in FC-40 with 2%, 1%, and 0.1% (w/w) surfactant, respectively. With 2% and 1% surfactant, the main peak in

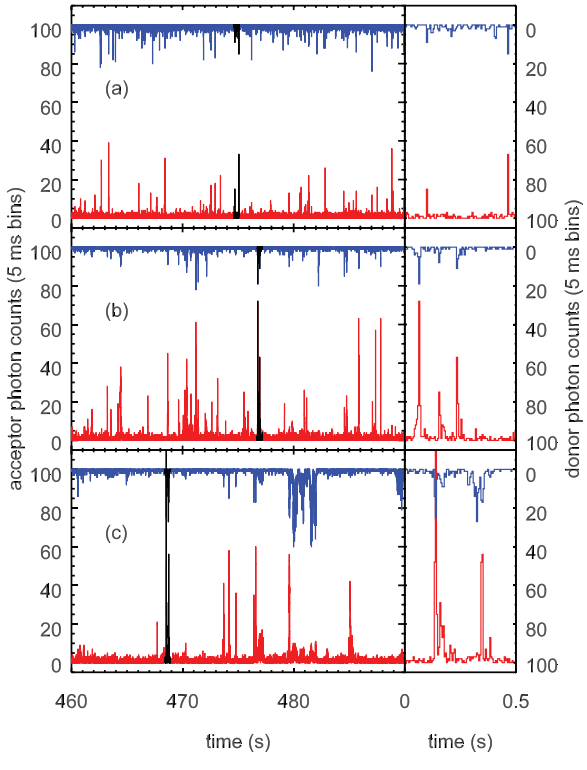

FIG. 1. A comparison of fluorescence from doubly labeled RNA duplexes (a) in solution (b) confined in droplets diffusing in FC-77 and (c) confined in droplets diffusing in FC-40. The acceptor channel is plotted in red, and the donor-channel is plotted upside-down in blue, with the associated axis label on the right. A 30 s portion of the 25–75 min long datasets are shown on the left; the small panels on the right are an 0.5 s expansion of the data colored black in the left panel.

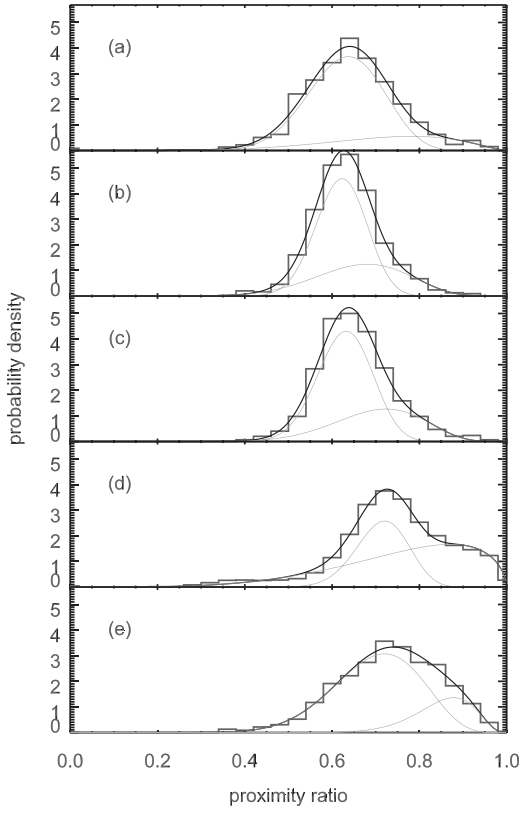

FIG. 2. Proximity histograms and fits for RNA (a) in solution at pH 7.8 with $N_{th} = 25$; (b) in droplets in FC-40 with 2% (w/w) surfactant and $N_{th} = 75$; (c) in droplets in FC-40 with 1% (w/w) surfactant and $N_{th} = 75$; (d) in droplets in FC-40 with 0.1% (w/w) surfactant and $N_{th} = 50$; (e) in solution at pH 5 with $N_{th} = 60$. See Table I for fit parameters.

TABLE I. Statistics and best fit parameters for the proximity histograms of Fig. 2. N_{th} is the threshold number of photons per bin, Fig. is the corresponding figure, A is the amplitude of the beta PDF, μ and β are the beta PDF parameters defined in the supplementary material,[8] $\langle P\rangle$ is the mean proximity ratio, σ_d and σ_s are the actual and shot-noise limit of the peak standard deviations, bins are the number of bins under the peak, and $\langle N_t\rangle$ is the mean number of photons per bin for that peak.

$\langle N_{th}\rangle$	Fig.	A	α	β	$\langle P\rangle$	σ_d	σ_s	Bins	$\langle N_t\rangle$
25	1(a)	0.80	19.63	11.61	0.628	0.094	0.083	1169	37.0
25	1(a)	0.20	6.32	2.49	0.718	0.149	0.078	303	37.7
75	1(b)	0.67	43.39	26.64	0.620	0.057	0.050	898	99.6
75	1(b)	0.33	13.04	6.64	0.663	0.106	0.048	472	100.5
75	1(c)	0.68	37.28	22.10	0.628	0.061	0.048	499	104.5
75	1(c)	0.32	14.20	6.05	0.701	0.108	0.046	241	104.5
50	1(d)	0.39	40.65	16.39	0.713	0.067	0.052	2055	85.1
50	1(d)	0.61	5.00	1.59	0.759	0.162	0.049	3369	87.0
60	1(e)	0.78	14.24	6.15	0.699	0.102	0.052	449	83.3
60	1(e)	0.22	22.67	4.00	0.850	0.067	0.040	126	83.8

the droplet histogram has $\langle P\rangle$ that is indistinguishable from that of the pH 7.8 solution data within the ± 0.01 uncertainty attributable to drift in the optics. However, the width of the histograms, which determines statistical uncertainty and the ability to discern heterogeneous populations, is substantially narrower for droplet data. This is a result of the increase in signal afforded by droplet confinement, which allowed a threefold increase in N_{th} over that of the solution data (Table I). A homogeneous peak in the proximity histogram (i.e., from a Poisson emitter) has a shot-noise limited variance[13] $\sigma_s^2 = [\langle P\rangle(1-\langle P\rangle)]/\langle N_t\rangle$. The factor of 2.6 increases in $\langle N_t\rangle$ gave a 60% decrease in σ_s.

In all cases, the standard deviation of the distributions, σ_d, is larger than σ_s (Table I). In general we attribute this, and the need for more than one beta PDF, to photophysical transitions which are known to heterogeneously broaden proximity histograms of cyanine dyes.[14]

All previous reports of spFRET from droplet-confined molecules[3,15,16] used optically trapped droplets and the water-soluble surfactant Triton X-100. In these conditions,[16] and at 0.1% fluorinated surfactant, FRET in droplets, Fig. 2(d), differs dramatically from solution FRET near neutral pH. The histogram is both shifted from, and more distinctly heterogeneous than, that of the pH 7.8 solution data. For the peak at lower P, repetitions of the low-surfactant droplet measurements (e.g., Fig. S2)[8] gave the same $\langle P\rangle$ within the ± 0.01 uncertainty. The second population had larger $\langle P\rangle$ and smaller σ_d for FC-77 than FC-40, Table S1.[8] The relative amplitude of the two peaks varied substantially; in rare cases, the higher FRET peak was the larger of the two (Fig. S2).[8] This RNA molecule has only one structure and photophysical effects should not cause such an obvious heterogeneity.

In searching for an explanation for the FRET shift of Fig. 2(d), we discovered that FRET for this system is pH dependent. Fig. 2(e) is a proximity histogram for RNA in solution at pH 5 that shows a similar shift in FRET; pH 4, 5, and 6 FRET data were indistinguishable (Fig. S3).[8] As discussed below, we also discovered that the low-surfactant droplets are acidic; we believe this explains the observed shift of the proximity ratio in droplets.

However, with values of N_{th} chosen to give similar values of $\langle N_t\rangle$, Figs. 2(d) and 2(e), we see immediately that the two proximity histograms still differ, with a more obvious splitting of the peak in the droplet data. Hypothesizing that the droplet interface might play a role in this difference, we looked for a correlation between proximity ratio and droplet size using photon-burst time length[8] as a proxy for size. Pearson's coefficients for burst time and $\langle P\rangle$ in a burst were between -0.1 and $+0.1$, indicating no correlation. However, the use of burst length as a proxy for size is imperfect; we cannot rule out that surface effects play a more subtle role.

We propose that changes in the Förster radius $R_F^6 = 9c^4 J\eta_D\kappa^2/8\pi n^4$, resulting from a modified pH in low-surfactant droplets, can account for the observed shift in $\langle P\rangle$. Here, n is the solvent's refractive index, c is the speed of light, η_D is the quantum yield of the donor dye in the absence of the acceptor, κ is the orientation term in a dipole-dipole interaction, and J is a spectral overlap integral. A spectral shift large enough to substantially change J would likely degrade the fluorescence signal into either the donor or the acceptor channel: instead, the brightness of droplet-confined dyes increases in both channels at low surfactant concentration, Fig. 3. The index difference between FC-40 (FC-77) and water is small, only 0.04 (0.05), and so it cannot significantly affect R_F or dye lifetime. This leaves changes in η_D and/or κ as potential causes of the shift in FRET. Both of these parameters are sensitive to changes of the dye conformation on RNA, which plausibly depends on pH.

Cyanine dyes are insensitive to changes in pH between 4 and 10.[17] However, the phosphates along the RNA backbone, which carry a double negative charge at pH 7, become

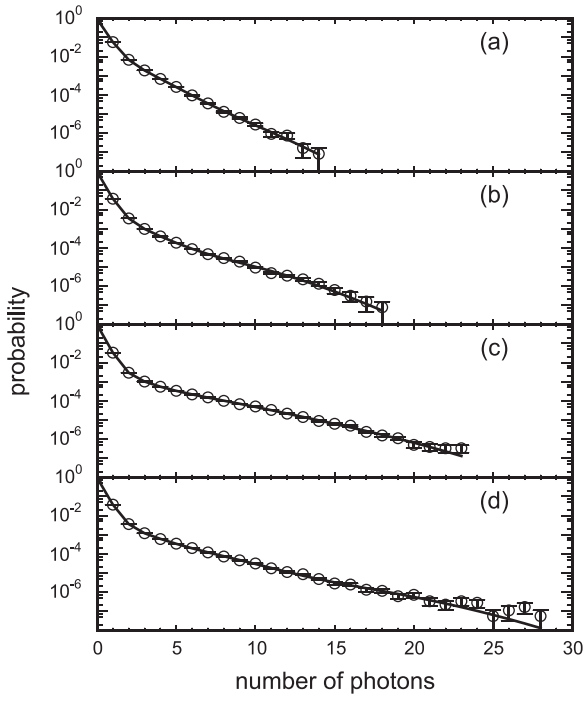

FIG. 3. PCH for donor-only-labeled RNA (a) in solution at pH 7 with a two species fit (line) with $\chi^2 = 0.7$; (b) in solution at pH 4 with a three species fit (line) with $\chi^2 = 1.3$; (c) in droplets in FC-77 and 0.1% surfactant with a three species fit (line) with $\chi^2 = 1.1$; and (d) in droplets in FC-40 and 0.1% surfactant with a three species fit (line) with $\chi^2 = 1.4$. χ^2 is calculated per degree of freedom and the bin time is 200 μs.

singly ionized near pH 6. Also, while most ribonucleotides have a $pK_a < 4$, cytidine monophosphate has a pK_a of 4.5; the phosphate backbone further increases the pK_a.[18] The RNA used here was studied using MD simulations, which showed that the dyes are primarily base-stacked on the ends of the duplex at neutral pH.[9] The RNA has two C-G pairs at each end, and it is possible that protonation occurring at lower pH causes fraying of the RNA or otherwise affects the stacking of the dyes on the RNA. Should fraying occur, cyanine dyes can intercalate into single strands, becoming substantially brighter (larger η_D).[19] It seems likely that the shift in FRET at low pH occurs due to a modified interaction between the dyes and the RNA that causes either a change in the dye brightness (which changes R_F) and/or a change in the interdye distance and orientation.

The proposed change in brightness was indeed observed using photon-counting histograms[20,21] (PCHs) of donor-only (Cy3) labeled RNA. The PCHs shown in Fig. 3 were taken on the same day under identical conditions with an excitation power of 50 μW.[8] For RNA in solution at pH 7, Fig. 3(a), the data are fit well by two species, presumably Cy3 isomers but possibly different conformations of Cy3 on the RNA, one with roughly twice the brightness and $<10\%$ the population of the other. Similar results were obtained at pH 7.8. Below pH 7 a new, brighter species emerges: three populations are required for a good fit. In solution at pH 4, Fig. 3(b), this new species is roughly eight times brighter than the dimmest species and comprises roughly 4% of the population. For droplets with 0.1% (w/w) surfactant, the situation is similar, Figs. 3(c) and 3(d); the new species is 5 to 6 times brighter than the dimmest species, and comprises at most 5.5% of the population. Differences between FC-77 and FC-40 are mostly insignificant; a complete set of PCH fitting parameters is given in Table SIII.[8]

Using pH sensing dyes, we confirmed that a non-ionic surfactant affects the pH in droplets, contrary to expectations. Starting with buffer at pH 7.8, droplets with 0.1% (w/w) surfactant had a confined-phase pH of 5.5, while above 1% surfactant the pH was near 7.3. Details will be reported elsewhere. The acidity of small water droplets with little or no surfactant was unexpected but should not be surprising. The zeta potential of particles, oil droplets, and air bubbles in pure water is known to be negative, a phenomenon widely ascribed to the autolysis of water and sequestration of hydroxide ions near or on the water boundary.[22] It has been shown that for oil-in-water emulsions, as the interfacial area increases (e.g., by decreasing droplet size), the pH of the aqueous phase decreases.[23] To maintain the pH of the continuous phase, it is necessary to titrate in enough NaOH to provide one OH- for every 3 nm^2 of surface. For a 100 nm diameter droplet, this corresponds to about 4×10^4 hydroxides sequestered at or very near the surface, more than enough to account for the observed change in the pH of the confined phase.

In conclusion, FRET in droplets with $\geq 1\%$ surfactant offers better signal to noise and is otherwise the same as FRET from molecules unconfined in solution. With 0.1% surfactant, droplets become acidic and $\langle P \rangle$ exhibits a shift that is similar in droplets and in bulk solution at low pH.

However, FRET from RNA confined in low surfactant droplets has greater heterogeneity than is observed in solution at low pH. One plausible hypothesis is that the kinetics are different. If the two populations seen in the proximity histograms represent the same dye isomers or dye conformations on RNA, then the more distinct splitting in Fig. 2(d) might indicate that kinetic transitions are slower in droplets than in bulk solution. When transitions are fast compared to the bin time, heterogeneities are washed out. Further investigation of kinetics in droplets would be needed to test this hypothesis. It seems likely that interactions at the water boundary play a role. Even if a droplet is at neutral pH, there will be a space charge layer near the surface. This might affect the kinetics, as well as the rotational and translational diffusion of the molecule.

The authors thank John Randolph at Glen Research, Brian Hutchison at RainDance Technologies, Anthony Dinsmore, Adrian Parsegian, and Rudi Podgornik at UMass for useful and illuminating discussion. This work was funded by NSF MCB-0920139 and NSF DBI-1152386.

[1]D. Nettels and B. Schuler, "Single-molecule FRET of protein-folding dynamics," in *Single-molecule Biophysics: Experiment and Theory*, Advances in Chemical Physics Vol. 146, edited by T. Komatsuzaki, M. Kawakami, S. Takahashi, H. Yang, and R. J. Silbey (Wiley, 2012), pp. 23–48.
[2]P. Li and L. Goldner, "Application of single-molecule fluorescence in RNA biology," in *RNA Nanotechnology*, edited by B. Wang (Pan Stanford, 2014), pp. 185–212.
[3]J. E. Reiner, A. M. Crawford, R. B. Kishore, L. S. Goldner, K. Helmerson, and M. K. Gilson, "Optically trapped aqueous droplets for single molecule studies," Appl. Phys. Lett. **89**, 013904 (2006).
[4]E. Boukobza, A. Sonnenfeld, and G. Haran, "Immobilization in surface-tethered lipid vesicles as a new tool for single biomolecule spectroscopy," J. Phys. Chem. B **105**, 12165–12170 (2001).
[5]J. Tang, A. M. Jofre, R. Kishore, J. E. Reiner, M. E. Greene, G. M. Lowman, J. S. Denker, C. Willis, K. Helmerson, and L. S. Goldner, "Generation and mixing of subfemtoliter volume aqueous droplets on demand," Anal. Chem. **81**, 8041–8047 (2009).
[6]J. Tang, A. M. Jofre, G. M. Lowman, R. B. Kishore, J. E. Reiner, K. Helmerson, L. S. Goldner, and M. E. Greene, "Green fluorescent protein in inertially injected aqueous nanodroplets," Langmuir **24**, 4975–4978 (2008).
[7]A. Jofre, J. Y. Tang, M. E. Greene, G. M. Lowman, N. Hodas, R. B. Kishore, K. Helmerson, and L. S. Goldner, "Hydrosomes: Femtoliter containers for fluorescence spectroscopy studies," Proc. SPIE **6644**, 66440E (2007).
[8]See supplementary material at http://dx.doi.org/10.1063/1.4921202 for details of the methodology and additional figures and tables.
[9]P. Milas, B. D. Gamari, L. Parrot, B. P. Krueger, S. Rahmanseresht, J. Moore, and L. S. Goldner, "Indocyanine dyes approach free rotation at the 3′ terminus of A-RNA: A comparison with the 5′ terminus and consequences for fluorescence resonance energy transfer," J. Phys. Chem. B **117**, 8649–8658 (2013).
[10]C. E. Aitken, R. A. Marshall, and J. D. Puglisi, "An oxygen scavenging system for improvement of dye stability in single-molecule fluorescence experiments," Biophys. J. **94**, 1826–1835 (2008).
[11]C. Holtze, A. C. Rowat, J. J. Agresti, J. B. Hutchison, F. E. Angilè, C. H. J. Schmitz, S. Köster, H. Duan, K. J. Humphry, R. A. Scanga, J. S. Johnson, D. Pisignano, and D. A. Weitz, "Biocompatible surfactants for water-in-fluorocarbon emulsions," Lab Chip **8**, 1632–1639 (2008).
[12]B. D. Gamari, D. Zhang, R. E. Buckman, P. Milas, J. S. Denker, H. Chen, L. Hongmin, and L. S. Goldner, "Inexpensive electronics and software for photon statistics and correlation spectroscopy," Am. J. Phys. **82**, 712–722 (2014).
[13]I. V. Gopich and A. Szabo, "Theory of single-molecule fret efficiency histograms," in *Single-molecule Biophysics: Experiment and Theory*,

Advances in Chemical Physics Vol. 146, edited by T. Komatsuzaki, M. Kawakami, S. Takahashi, H. Yang, and R. Silbey (John Wiley & Sons, Inc., 2012), pp. 245–297.
[14]S. Kalinin, E. Sisamakis, S. W. Magennis, S. Felekyan, and C. A. M. Seidel, "On the origin of broadening of single-molecule fret efficiency distributions beyond shot noise limits," J. Phys. Chem. B **114**, 6197–6206 (2010).
[15]S. Hicks, J. Case, and A. Jofre, "Conformational diversity of short DNA duplex," J. Phys. Chem. B **114**, 15134–15140 (2010).
[16]L. S. Goldner, A. M. Jofre, and J. Y. Tang, "Droplet confinement and fluorescence measurement of single molecules," Methods Enzymol. **472**, 61–88 (2010).
[17]R. B. Mujumdar, L. A. Ernst, S. R. Mujumdar, C. J. Lewis, and A. S. Waggoner, "Cyanine dye labeling reagents—sulfoindocyanine succinimidyl esters," Bioconjugate Chem. **4**, 105–111 (1993).
[18]V. A. Bloomfield, D. M. Crothers, and J. I. Tinoco, "Bases, nucleosides, and nucleotides," in *Nucleic Acids: Structures, Properties, and Functions* (University Science Books, Sausalito, CA, 2000), pp. 13–43.
[19]J. B. Randolph and A. S. Waggoner, "Stability, specificity and fluorescence brightness of multiply-labeled fluorescent DNA probes," Nucleic Acids Res. **25**, 2923–2929 (1997).
[20]Y. Chen, J. D. Muller, P. T. C. So, and E. Gratton, "The photon counting histogram in fluorescence fluctuation spectroscopy," Biophys. J. **77**, 553–567 (1999).
[21]B. Huang, T. Perroud, and R. Zare, "Photon counting histogram: One-photon excitation," ChemPhysChem **5**, 1523–1531 (2004).
[22]J. K. Beattie, A. N. Djerdjev, and G. G. Warr, "The surface of neat water is basic," Faraday Discuss. **141**, 31–39 (2009).
[23]J. Beattie and A. Djerdjev, "The pristine oil/water interface: Surfactant-free hydroxide-charged emulsions," Angew. Chem. Int. Ed. **43**, 3568–3571 (2004).